

Curriculum-based Sample Efficient Reinforcement Learning for Robust Stabilization of a Quadrotor

Fausto Mauricio Lagos Suarez¹, Akshit Saradagi, Vidya Sumathy,
Shruti Kotpalliwar and George Nikolakopoulos

Abstract—This article introduces a novel sample-efficient curriculum learning (CL) approach for training an end-to-end reinforcement learning (RL) policy for robust stabilization of a Quadrotor. The learning objective is to simultaneously stabilize position and yaw-orientation from random initial conditions through direct control over motor RPMs (end-to-end), while adhering to pre-specified transient and steady-state specifications. This objective, relevant in aerial inspection applications, is challenging for conventional one-stage end-to-end RL, which requires substantial computational resources and lengthy training times. To address this challenge, this article draws inspiration from human-inspired curriculum learning and decomposes the learning objective into a three-stage curriculum that incrementally increases task complexity, while transferring knowledge from one stage to the next. In the proposed curriculum, the policy sequentially learns hovering, the coupling between translational and rotational degrees of freedom, and robustness to random non-zero initial velocities, utilizing a custom reward function and episode truncation conditions. The results demonstrate that the proposed CL approach achieves superior performance compared to a policy trained conventionally in one stage, with the same reward function and hyperparameters, while significantly reducing computational resource needs (samples) and convergence time. The CL-trained policy’s performance and robustness are thoroughly validated in a simulation engine (Gym-PyBullet-Drones), under random initial conditions, and in an inspection pose-tracking scenario. A video presenting our results is available at <https://youtu.be/9wv6T4eezAU>.

I. INTRODUCTION

In the recent years, Reinforcement Learning (RL) has emerged as an appealing control design tool for engineers, with and without formal training in machine learning and automatic control. This is especially true in the design of autonomy for Quadrotors, where RL is being used to learn policies for path planning, navigation, and control [1]. RL has proven particularly effective in tackling complex aerial control tasks that are challenging for classical system-theoretic approaches [2]. In RL, an agent learns a specific behavior in a model-free fashion, by interacting with its environment, by taking actions, and receiving numeric rewards

*This work has been funded by the European Union’s Horizon Europe Research and Innovation Program, under the Grant Agreement No. 101119774 SPEAR.

¹This research was conducted using the resources of High Performance Computing Center North (HPC2N). Additionally, the RL-training were enabled by resources provided by the National Academic Infrastructure for Supercomputing in Sweden (NAISS), partially funded by the Swedish Research Council through grant agreement no. 2022-06725.

¹Fausto Lagos is the corresponding author of the article faulag@ltu.se. The authors are with the Robotics and AI group, in the Department of Computer Science, Electrical and Space Engineering at Luleå University of Technology, Sweden.

that indicate the effectiveness of the actions in achieving the desired behavior [3]. This makes RL well-suited for complex learning tasks involving UAVs, where precise modeling of the interaction between the UAV’s nonlinear dynamics and the surrounding aerial flows is highly challenging, especially for soft and unconventional drone designs [4].

Although recent RL demonstrations portray RL to be almost akin to plug-and-play, researchers in academia and industry recognize the significant human time and effort involved in solving complex control problems using RL, even when powerful computing clusters are employed. It is not uncommon for even experienced Ph.D students in academia and trained personnel in industry to spend several months in iteratively perfecting RL training, with reward design and hyperparameter optimization accounting for a major part of the time and effort. Although using modern GPUs and extreme parallelization in training, millions of time steps (samples) of training can be achieved in minutes [5] [6], RL training for UAVs is still computationally intensive and time-consuming, which underscores the need to investigate the fundamental challenge of sample-efficiency in order to develop sample-efficient RL training methods.

Recent literature on RL-based control for Quadrotors has explored diverse aspects: design of Gym environments for parallelized training [7] [8], training setups for zero-shot sim-2-real transfer [9], exploration of the right action and observation spaces [10] [11], design of reward functions to achieve specific aerial objectives [12], generalization of RL training to multiple Quadrotors through domain randomization [13], improvements to training algorithms such as the Proximal Policy Optimization (PPO) algorithm for improved learning stability [14], exploration of different training algorithms such as DDPG, TRPO, PPO for quadrotor control [15] etc. Additionally, [16] introduced an RL-based controller capable of stabilizing a Quadrotor from extreme initial conditions, such as manual tossing, which is relevant in the context of this article.

It is worth noting that, in the literature alluded to so far, a conventional one-stage training approach has been utilized, with no mention of the sample efficiency of the training process and the significant computation and wall-clock time spent in tuning the RL training. In this context, this article draws inspiration from bio-inspired curriculum learning and proposes a light, structured and modular three-stage RL-training workflow to achieve robust stabilization for a Quadrotor (position and yaw) starting from random initialization in position, orientation, and non-zero linear and

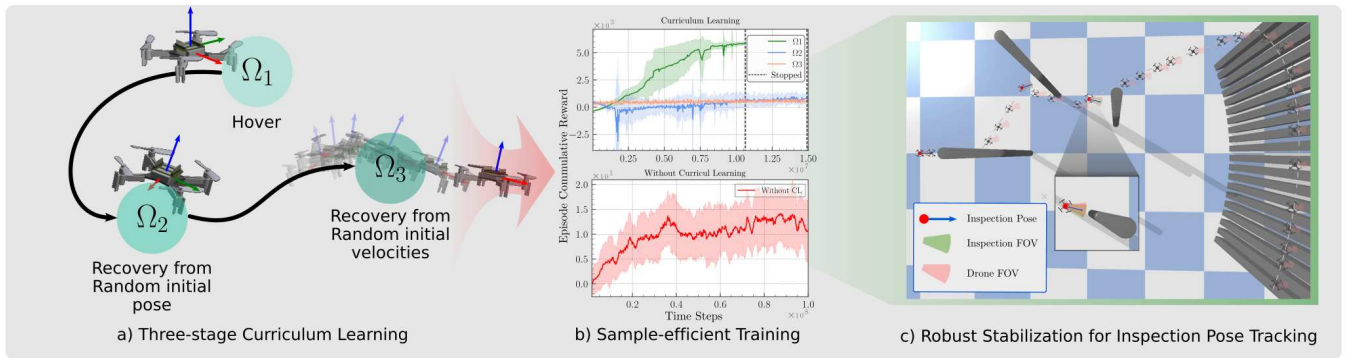


Fig. 1: A curriculum learning-inspired computationally-efficient three-stage RL training approach, to learn a policy for quadrotor control, while meeting pre-specified transient and steady-state requirements from aerial inspection missions.

angular velocities. This learning objective, highly relevant in aerial inspection and monitoring applications, is challenging for single-stage training commonly used in RL literature, which requires several hundred million time steps in one-stage training [17]. Curriculum learning, which has gained popularity in legged robotics [18] and autonomous robotics [19], has not yet been exploited in RL-based quadrotor control literature. This is mainly due to the emergence of GPU-aided Gyms, which have significantly reduced the time between two tuning runs.

Contributions: Given the premise, the contributions of this article (depicted pictorially in Fig. 1) are presented next. This work presents a novel three-stage Curriculum Learning (CL) methodology for training an RL agent to achieve robust stabilization of a Quadrotor (position and yaw). The focus on sample-efficient training and the goal of achieving pre-specified settling time and steady-state requirements sets this article apart from existing literature. 1) The proposed curriculum (Section III), wherein the domain of quadrotor initializations is progressively expanded in three stages, is designed while taking into account the underactuated nature of the Quadrotor and the coupling between the translational and rotational degrees-of-freedom. This is unlike in [5], wherein the curriculum is set up to sequentially change the weights in the reward functions. 2) This work proposes a reward function and episode truncation conditions to achieve pre-specified settling time and steady-state requirements, motivated by the needs of the aerial inspection and monitoring applications. 3) The results (Section V) demonstrate that the proposed CL-training significantly enhances the sample efficiency of the training process compared to single-stage training, which fails to achieve the considered learning objective, even with extended training periods, with the same reward function and hyperparameters of the training algorithm. The robustness of the CL-trained policy is validated through extensive testing from a diverse set of initial conditions and in an inspection pose tracking scenario.

II. PROBLEM FORMULATION

A Quadrotor is an underactuated aerial system with six degrees-of-freedom (DOF): three translational $((x, y, z) \in$

\mathbb{R}^3) and three rotational $(\phi, \theta, \psi \in \mathbb{S}^1 \times \mathbb{S}^1 \times \mathbb{S}^1)$. The Quadrotor is influenced by four control inputs supplied to the four motors M1-M4. The motors produce upward thrust and the roll, pitch, and yaw rotations necessary for aerial mobility. In this article, a Crazyflie 2.1 (shown in Figure 2) in \times configuration is considered. Mathematical modeling of the Quadrotor dynamics can be found in [20]. **Problem**

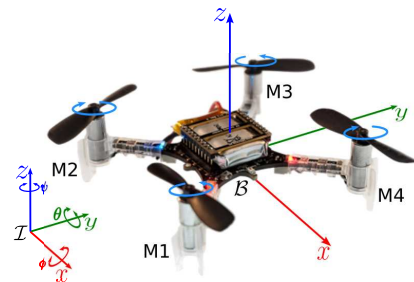


Fig. 2: The Crazyflie Quadrotor.

statement. The training of an end-to-end RL policy to achieve robust stabilization of a Quadrotor, with acceptable performance levels, requires millions of interactions [21] with the training environment, despite the availability of Gym environments aided by high-performance Graphics Processing Units (GPUs). To address this challenge, this work considers the problem of developing a methodology for RL training that can be a sample-efficient alternative to the ubiquitous one-stage training. The learning objective is to achieve robust stabilization of a Quadrotor through direct control of the Quadrotor's RPMs (end-to-end), from random initial states (including non-zero velocities). Driven by the rigorous demands on Quadrotor stability in aerial inspection missions, the objective also includes satisfying desired control-theoretic performance metrics such as settling time and steady-state accuracy in both position and yaw-orientation. For validation, the performance specifications are set to: i) settling time of less than 5 seconds, ii) positional steady-state error within 2.5 cm of the target position, and iii) yaw-tracking error within 2° of the commanded target yaw orientation.

III. CURRICULUM LEARNING METHODOLOGY

Curriculum learning involves three key components: sub-task generation, sequencing, and transfer learning. This approach decomposes a complex target task into a series of sub-tasks, progressively transferring knowledge through multiple learning stages until the target is achieved [22]. This section introduces a sequenced three-stage curriculum, designed to enhance sample efficiency of the RL training process for Quadrotor control. In synthesizing a sequence of three sub-tasks, the Quadrotor’s under-actuated nature and the coupling between different degrees-of-freedom of a Quadrotor are taken into account. The training initially focuses on the task of achieving stable hovering from a fixed position. The task difficulty gradually increases in two additional stages, where random initialization in positions/orientations and velocities (both linear and angular), respectively, are introduced along with the requirement for achieving 0° as target yaw. In general, sub-tasks may differ from the final task in terms of state/action space, reward function, or transition dynamics [23] [24]. In this work, we maintain a consistent reward function structure across all sub-tasks, but sequentially expand the domain of initialization of the Quadrotor, thereby altering the environment within the Markov Decision Process (MDP). The **first sub-task** (Ω_1) focuses on achieving a target hover position at $(x(t), y(t), z(t)) = (0, 0, 1)$, starting from the fixed position $(x(0), y(0), z(0)) = (0, 0, 0)$. In this stage, the policy is trained to control the drone to take off and maintain the target position, which essentially involves learning to use the same RPM values for all four motors. Such a policy is better suited to learning the sub-task Ω_2 presented next, compared to a policy that is randomly initialized (as in one-stage training). The **second sub-task** (Ω_2) increases task complexity by requiring the drone to reach $(x(t), y(t), z(t)) = (0, 0, 1)$ and $\psi(t) = 0$, from random initial positions within a cylinder of 2 meters radius and 2 meters height, and random initial attitudes with roll and pitch angles in a safe range of $[-15^\circ, 15^\circ]$ and yaw angle in a range of $[-180^\circ, 180^\circ]$. This task emphasizes learning the coupling between the x and y degrees-of-freedom and the roll (ϕ) and pitch (θ) rotations. A policy that achieves task Ω_2 is well placed to learn the final task Ω_3 presented next, compared to a policy that is randomly initialized (as in one-stage training). The **third sub-task** (Ω_3), which corresponds to the learning objective of robust stabilization, further increases difficulty by introducing random initial linear velocities within the range of $[-1, 1]$ meters per second and angular velocities within the range of $[-1, 1]$ radians per second, in addition to random initial positions and orientations. Here, the policy learns to command the four motors to achieve the desired position and yaw, while correcting for deviations induced by random initial velocities. A pictorial illustration of the three-stage curriculum is presented in Fig. 3. To evaluate the gains in sample efficiency and convergence time of the proposed curriculum learning against the baseline of one-stage training, the number of time steps and wall-clock time required to achieve the target task are used as

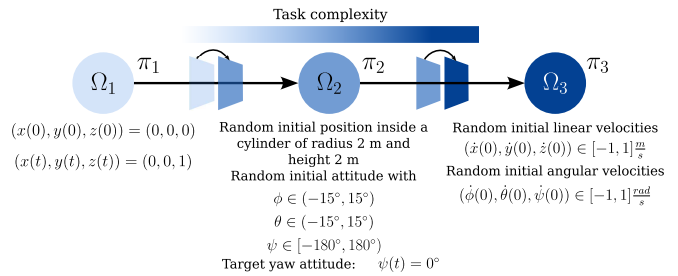


Fig. 3: The sequence of tasks in the proposed three-stage curriculum learning, showing the evolution of the task complexity and variations in the domain of initialization.

metrics in Section V. The evaluation focuses on showcasing the ability of the curriculum-trained policy to achieve the learning objective while yielding significant reduction in training time and enhanced sample efficiency.

IV. REINFORCEMENT LEARNING SETUP

In the reinforcement learning framework, the control of a Quadrotor is modeled as a Markov Decision Process and represented as a tuple of five elements $(\mathbb{E}, \pi, \mathbb{A}, \mathbb{S}, \mathbf{R})$, where \mathbb{E} is the environment (the simulation engine *Gym-PyBullet-Drones* in this case), \mathbb{A} is the set of actions, \mathbb{S} and \mathbf{R} are the current state (observation) and rewards returned by the environment respectively, and π is the policy (a neural network) in charge of taking control decisions (mapping observations to actions).

A. Observation and action spaces

In this work, we consider a 12-dimensional observation space consisting of the position $[x \ y \ z] \in \mathbb{R}^3$, the Euler angles $[\phi \ \theta \ \psi] \in \mathbb{S}^1 \times \mathbb{S}^1 \times \mathbb{S}^1$, the linear velocities $[\dot{x} \ \dot{y} \ \dot{z}] \in \mathbb{R}^3$ and the angular velocities $[\dot{\phi} \ \dot{\theta} \ \dot{\psi}] \in \mathbb{R}^3$. The rotor speeds R_1, \dots, R_4 (in RPM) of the propellers constitute the action space. The end-to-end reinforcement learning policy π directly maps the observation space (states) to the action space (RPMs of the motors). The Crazyflie Quadrotor considered in this work allows for direct control with the RPMs of the motors.

B. Reward shaping

The goal of an RL algorithm is to train an agent to obtain the most discounted cumulative reward over time. Although several works in literature (such as [25]) suggest having a simple reward function based on just the error in position and velocities, simple rewards lead to sample inefficiency, as the policy explores without adequate feedback, and are not suitable for problems that go beyond hovering. To develop an RL policy that yields high accuracy, stability, and robustness, while having good sample efficiency in training, a reward function that encodes such expectations must be crafted. In this article, we design an additive reward function that penalizes excessive exploration, instability, and imprecision in reaching the target position and attitude, that are crucial for both robust stabilization and improved sample efficiency of

the training process. In this article, we propose the following reward function:

$$R(t) = 25 - 20T_e - 100E + 20S - 18w_e, \quad (1)$$

where the individual components are defined below. Although some of the terms are in fact penalties and not rewards, we use the term ‘reward’ without loss of generality.

Target reward (T_e): The target reward is a penalty proportional to the distance between the Quadrotor and the target position (T), and the difference between the target yaw and the current yaw. The penalty decreases as the Quadrotor nears the target configuration. The penalty is computed as:

$$T_e = ||[x_T \ y_T \ z_T] - [x \ y \ z]|| + |\psi_T - \psi|, \quad (2)$$

where the targets are indicated through a subscript.

Exploration reward (E): The exploration space for the policy is designed to be a cylinder, centered at the target position (T). In each episode, the cylinder’s radius is set to the distance between the center and the starting position of the quadrotor plus a tolerance δ_R , and the height is the target height z plus a tolerance δ_H . This bounded exploration space, along with the truncation conditions for each training episode, helps in lowering the overall training time, without compromising on the agent’s ability to explore adequately. The exploration reward (E) is defined as:

$$E = \begin{cases} 1 & d(C, T) > d(i, T) + \delta_R \vee C_z > T_z + \delta_H \\ -0.2 & \text{otherwise} \end{cases}, \quad (3)$$

where i , C and T refer to the initial, current and target positions, respectively.

Stability reward (S): To ensure that the drone achieves stability at the target position, we provide a positive reward when the drone is within Δ_p cm of the target position and the sum-of-squares of the roll and pitch angles are within Δ_a . Otherwise, the drone receives a penalty proportional to the sum of deviations in roll and pitch from zero. The stability reward (S) is defined as:

$$S = \begin{cases} 2 & d(C, T) < \Delta_p \wedge \phi^2 + \theta^2 < \Delta_a \\ -(\phi^2 + \theta^2) & \end{cases} \quad (4)$$

The parameter Δ_p represents the radius of a tolerance sphere centered at the target position and helps in imposing a pre-specified steady-state error, while Δ_a sets the tolerance on the final roll (ϕ) and pitch (θ) angles.

Navigation reward (w_e): To ensure smooth navigation from the starting position to the target position, we penalize significant changes in angular velocities. The penalty is proportional to the difference between the angular velocity in the previous time step and the current time step. The navigation reward (w_e) is calculated as

$$w_e = \sum_{i=1}^3 (w_{i_{t-1}} - w_{i_t})^2, \quad (5)$$

where $w \in \{\dot{\phi}, \dot{\theta}, \dot{\psi}\}$.

Episode length and Episode truncations: The episode length is set to the settling time specified in the performance requirements (5 seconds in the results). The stability reward in Equation 4 is designed to incentivize the policy to maintain Quadrotor stability beyond the episode length. In Equation 3, $\delta_R = 2.5$ cm is chosen as a tolerance margin for the radius of the cylinder. If at any moment of the episode, the distance to the target overshoots the radius of the cylinder plus δ_R , the episode is truncated. Although in the reward function, specific penalties for high roll or pitch angles are not imposed, episodes are truncated when the roll or pitch angle exceeds $\pm 15^\circ$.

V. PROCEDURE FOR SEQUENTIAL TRAINING

In this article, the standard implementation of the Proximal Policy Optimization (PPO) algorithm, considered a state-of-the-art RL algorithm [14], is used to train the curriculum learning policy.

Policy	MlpPolicy	Epochs	10
Learning rate	3×10^{-4}	Discount Factor (γ)	0.99
Batch Size	128	Episode Length	5 s

TABLE I: Parameters for the PPO algorithm.

Parameter	Notation	Value
Mass	m	$0.027 [Kg]$
Arm length	d	$39.73 \times 10^{-3} [m]$
Propeller radius	p	$23.1348 \times 10^{-3} [m]$
Moment of Inertial about x axis	I_{xx}	$1.395 \times 10^{-5} [Kg \times m^2]$
Moment of Inertial about y axis	I_{yy}	$1.436 \times 10^{-5} [Kg \times m^2]$
Moment of Inertial about z axis	I_{zz}	$2.173 \times 10^{-5} [Kg \times m^2]$

TABLE II: Physical parameters of the Crazyflie 2.x.

Training process and simulation engine. Table I presents the parameters used in the PPO algorithm and Table II presents the physical parameters for Crazyflie 2.x Quadrotor used for simulation.

For the training process, we used *Gym-PyBullet-Drones* [26], a gymnasium [27] environment that uses PyBullet Physics [28] as the physics engine and StableBaselines3 [29] as the library of reliable implementations of RL algorithms in PyTorch. *Gym-PyBullet-Drones* was developed to work directly with Crazyflie 2.0 in the \times and $+$ configurations, and allows for introducing obstacles into the training environment and during policy testing.

The actor (policy) neural network is a Multi-layered Perceptron (MLP) network [30] with four layers: the first is a layer of 12 inputs (the observation space), the two hidden layers have 64 fully connected nodes with tanh activation functions, and the last layer is a four-node layer (the action space). The critic (value function) network has the same architecture, except for the last layer, which is a one-node layer yielding the output of the value function. Figure 4 shows the RL training architecture, along with the configuration of the actor-critic neural networks used in this work. The training was executed on a single CPU on

a Compute-skylake Kebnekaise HPC2N node with an Intel Xeon Gold 6132 CPU and 192 GB RAM running 4 parallel environments.

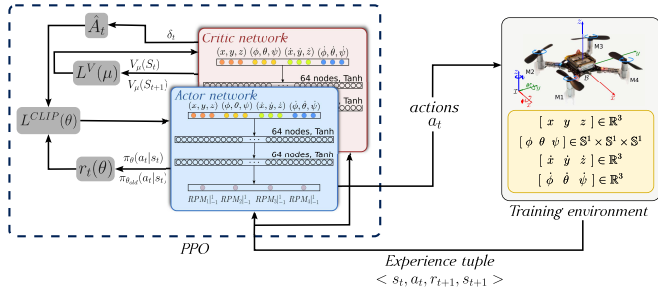


Fig. 4: Reinforcement Learning setup and configuration of the Neural Networks. The RL agent (actor network) interacts with the training environment by generating actions a_t , based on the current state s_t , provided by the environment. The critic network estimates the value function, $V(s_t)$, to evaluate the state. The experience tuple $\langle s_t, a_t, r_{t+1}, s_{t+1} \rangle$ is used to update both actor and critic networks through PPO’s objective function, including the clipped surrogate loss, $L_{CLIP}(\theta)$.

To demonstrate the effectiveness of the curriculum learning methodology in achieving the target task and to compare the performance with single-stage training, two agents were trained. The first agent was trained directly on the target task in a single stage (without curriculum learning), and the training process was monitored using the Episode Cumulative Reward (ECR) metric. Using the training setup from Section V, after 100 million time steps, which corresponds to more than 23 hours of computation, single-stage training failed to achieve the target task, which can be inferred from the consistently low ECR achieved by single-stage training (Figure 5).

The second agent was trained using the three-stage curriculum learning approach proposed in this article, which achieved the target task at the end of Ω_3 . The training process in each stage was monitored and stopped once the ECR stabilized for at least one million time steps. In Sub-task Ω_1 , the agent achieves higher cumulative rewards quickly, indicating excellent performance in learning to hover. This knowledge is then effectively transferred to subsequent tasks (Sub-task Ω_2 and Ω_3), which naturally exhibit lower cumulative rewards due to increased task difficulty introduced by random initial conditions and episode truncations. Table III presents a comparison of the time steps and wall-clock time required for single-stage training versus curriculum learning. Figure 5 provides a visual comparison of the ECR achieved by the policy trained in one stage versus the policy trained using curriculum learning.

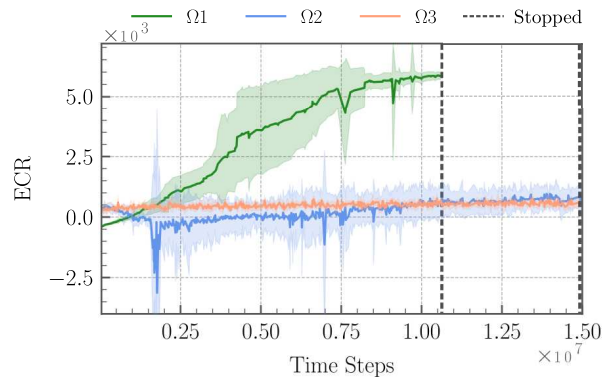
Both the curriculum learning and single-stage training approaches were trained utilizing the same neural network architecture and reward function structure. The evolution of training depicted in Figure 5 and the statistics presented in Table III clearly show the effectiveness of curriculum learning in improving sample efficiency. Curriculum learning allowed the agent to progressively learn increasingly difficult

stabilizing maneuvers, resulting in faster convergence and higher cumulative rewards compared to single-stage training.

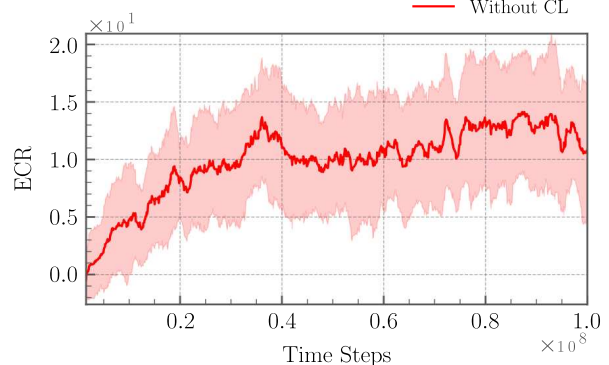
VI. TESTING OF THE CURRICULUM-TRAINED RL POLICY

Agent	Time steps	Wall clock
One Stage	100 million	23.4 hours
Sub-task Ω_1	11.5 million	3 hours
Sub-task Ω_2	15 million	4 hours
Sub-task Ω_3	15 million	4 hours
CL $\Omega_1 \rightarrow \Omega_3$	41.5 million	11 hours

TABLE III: Sample efficiency of Curriculum Learning vs one-stage training w.r.t time steps and wall clock time.



(a) Three-stage CL



(b) One stage training

Fig. 5: Episode Cumulative Reward (ECR) comparison between curriculum learning (a) and single-stage training (b).

The robustness and stability achieved by the curriculum-trained policy, is evaluated in two test scenarios: i) In the first, the performance of the policy in achieving a target position and orientation, starting from randomized position, orientation, and velocities is evaluated and ii) In the second, the accuracy in an inspection scenario, where the drone is required to reach a sequence of inspection view poses (positions with a specific orientation) is evaluated.

i) Robust stabilization: The performance of the CL-trained policy was evaluated by randomly setting the initial states of the drone and testing its ability to achieve the target configuration $(x, y, z, \phi, \theta, \psi) = (0, 0, 1, 0, 0, 0)$ and

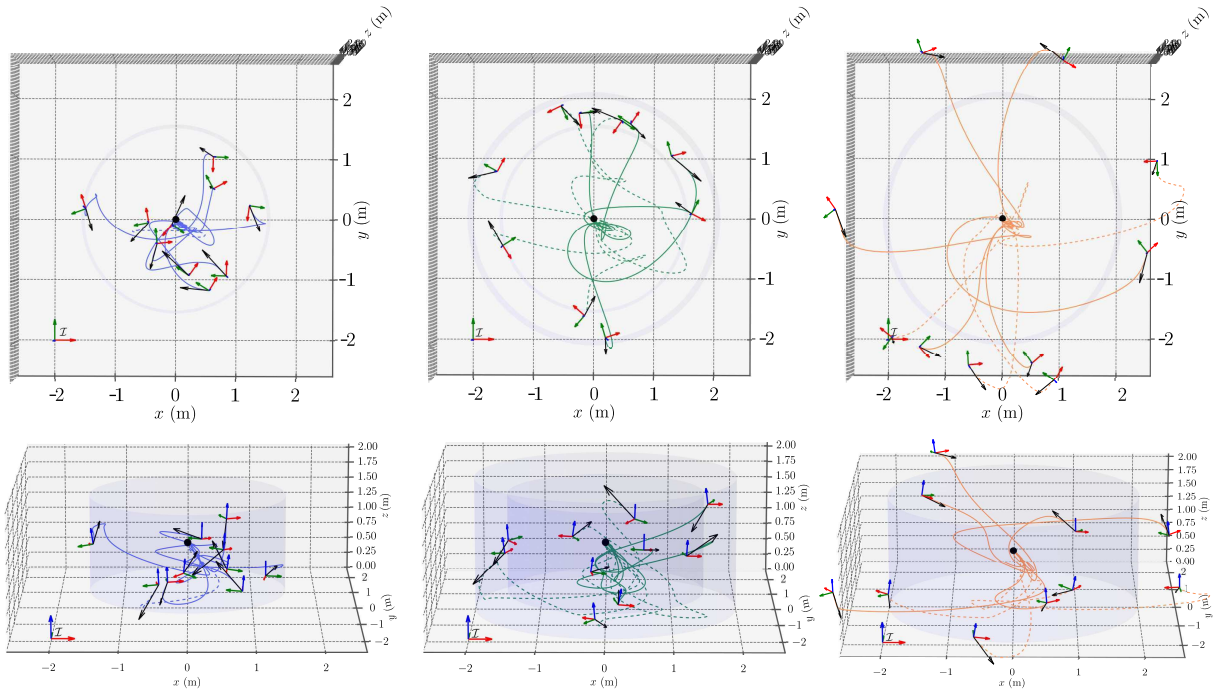


Fig. 6: Evaluation of the curriculum-trained policy over 30 trials with initial positions sampled from three regions. At each initial quadrotor position, the body frame indicates attitude and a black arrow denotes the randomized initial linear velocity, with length proportional to its magnitude; random nonzero angular velocities are also applied. Solid trajectories correspond to smooth maneuvers with small transients, whereas dashed trajectories indicate large transients that occur near the ground when compensating for large unfavorable initial velocities. In all cases, the drone reaches the target position.

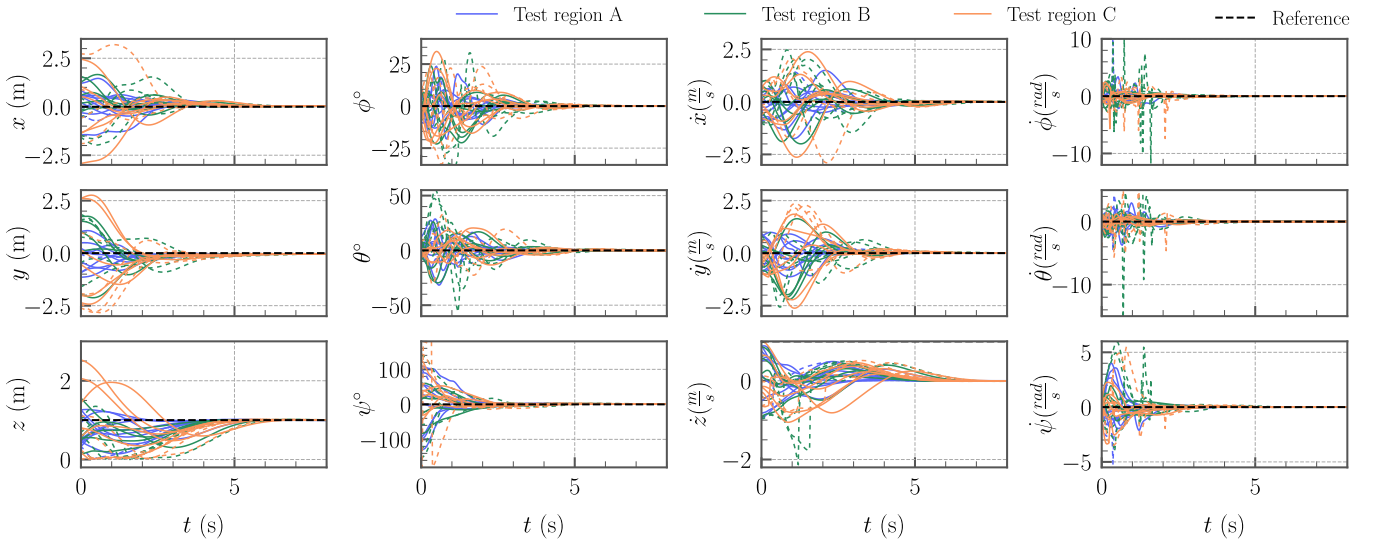


Fig. 7: Performance of the CL-trained policy in achieving robust stabilization from 30 randomized initial conditions. Trajectories with initialization in the three regions A, B and C are shown in different colors: inner cylinder (Region A, blue), annular region (Region B, green), and outer cylinder (Region C, orange). Dashed traces indicate large transients, where the drone reaches close to the ground (seen from the evolution of the z state), to overcome large initial velocities. The black dashed line represents the reference target values. The curriculum-trained policy consistently drives the system to the target position, from a diverse set of initial states.

$(\dot{x}, \dot{y}, \dot{z}, \dot{\phi}, \dot{\theta}, \dot{\psi}) = (0, 0, 0, 0, 0, 0)$. We conducted 30 trials, each lasting 8 seconds, starting from randomized initial positions, orientations, linear velocities, and angular velocities. The 30 initial conditions were split among three regions

shown in Figure 6: Test region A, which is a cylinder with radius 1.5 m and height 1.5 m; Test region B, which is an annular region with inner radius of 1.5 m, outer radius of 2 m, and height of 2 m; Test region C, which is a cylinder

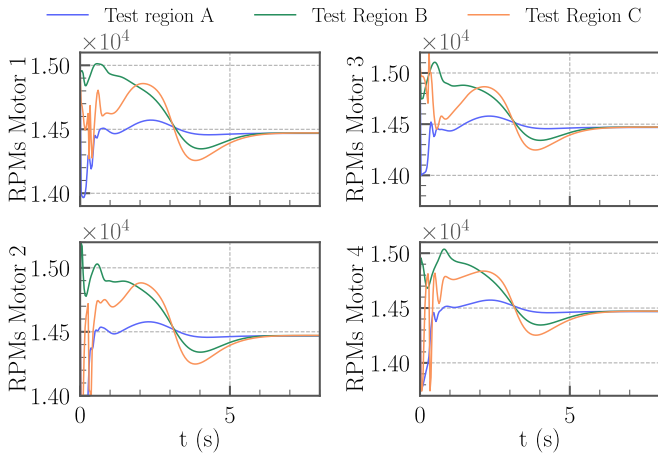


Fig. 8: RPMs commanded by the curriculum-trained policy for the four motors of the Crazyflie Quadrotor, when the Quadrotor is initialized in the regions A, B and C.

with a radius of 2 m and height of 2 m. For all the trials, the initial roll (ϕ) and pitch (θ) angles were randomized in the range $[-15^\circ, 15^\circ]$ and the yaw (ψ) angle in the range of $[-180^\circ, 180^\circ]$, the linear velocities were initialized in the range of $[-1, 1] \frac{m}{s}$ and the angular velocities in the range of $[-1, 1] \frac{rad}{s}$. In all scenarios, as can be seen in Figure 6, the drone successfully reached the target position, demonstrating the capability of the curriculum-trained policy in robustly stabilizing the Quadrotor at the target position.

In Figure 7, we plot the evolution of the Quadrotor’s position, orientation, linear velocity, and angular velocity from all 30 initial conditions. In most cases, the policy successfully negates the effect of non-zero initial linear and angular velocities and drives the Quadrotor to the target in less than five seconds, with smooth and safe transients. However, in five tests where the initial velocity was excessively high or the quadrotor was oriented away from the target, the drone exhibited complex and large transients, bringing the Quadrotor close to the ground, before driving it to the target configuration. In all 30 tests, the curriculum-trained policy consistently guided the drone to the target position with high accuracy, thus achieving robust stabilization of the Quadrotor from a diverse set of initial conditions. Figure 8 presents the motor RPMs generated by the curriculum-trained policy for three representative initial conditions from regions A, B, and C. In all three cases, the RPMs of all motors reach the steady-state hover RPMs.

ii) Inspection Scenario: A test scenario inspired by aerial inspection missions was designed to assess the robustness of the CL-trained policy in achieving a sequence of inspection view poses (target positions with target yaw angles). In this scenario, the drone is required to reach three columns placed at different locations and inspect points at different altitudes, and then move on to inspect a circular wall while maintaining its orientation aligned towards the wall by adjusting its yaw orientation. Although the CL-trained policy achieved zero yaw-orientation in all robust stabilization tests,

it was observed that it robustly tracks non-zero yaw-reference angles only from the set $[-25^\circ, 25^\circ]$. In this scenario, using the CL-policy, the drone achieved each inspection target point with reference yaw orientation chosen from the set $[-25^\circ, 25^\circ]$, exhibiting performance that aligns with the predefined performance specifications set in the problem definition (Section II) of less than 5 seconds of settling time, less than 2.5 cm in positional steady state error, and less than 2° error in yaw-tracking, while safely maintaining the roll and pitch angles between the safety boundaries of 15° (set in training to enable smooth movements).

The results presented so far demonstrate that the proposed curriculum learning approach, combined with the compounded reward function, allows the RL agent to achieve a high degree of stability, accuracy and robustness under complex initial conditions, including random linear and angular velocities. This suggests that the CL-trained agent has the potential to function as a reliable, general-purpose low-level controller for Quadrotors, subject to bridging the gap between simulation and real-world (sim2real) deployment.

VII. CONCLUSION AND FUTURE DIRECTIONS

This work proposed a sample-efficient three-stage curriculum learning methodology for efficiently and effectively training a reinforcement learning agent to accomplish robust stabilization for Quadrotors. An additive reward function was proposed to incorporate transient performance and steady-state accuracy requirements. From the results, it was concluded that curriculum learning was significantly more sample efficient compared to one-stage training (for the considered task and reward structure), which failed to achieve the learning objective even after 100 million time steps, with the same reward and PPO hyperparameters. The performance of the curriculum-trained RL policy was thoroughly tested in a physics-based simulator, from different initial conditions and in an inspection scenario requiring the policy to track a sequence of inspection view poses. The future work involves automating the curriculum setup and transferring the policy to real drones, thereby closing the simulation-to-reality gap.

REFERENCES

- [1] J. Alvarez, A. Belbachir, F. Belbachir, J. Chahal, A. Goudjil, J. Gustave, and A. Öztürk Suri, “Forest Fire Localization: From Reinforcement Learning Exploration to a Dynamic Drone Control,” *Journal of Intelligent & Robotic Systems*, vol. 109, no. 4, p. 83, Nov. 2023. [Online]. Available: <https://doi.org/10.1007/s10846-023-02004-z>
- [2] L. Antonyshyn and S. Givigi, “Deep Model-Based Reinforcement Learning for Predictive Control of Robotic Systems with Dense and Sparse Rewards,” *Journal of Intelligent & Robotic Systems*, vol. 110, no. 3, p. 100, Jul. 2024. [Online]. Available: <https://doi.org/10.1007/s10846-024-02118-y>
- [3] R. Sutton and A. Barto, *Reinforcement Learning, second edition: An Introduction*, ser. Adaptive Computation and Machine Learning series. MIT Press, 2018. [Online]. Available: <https://books.google.se/books?id=sWV0DwAAQBAJ>
- [4] D. Zhang, A. Loquercio, J. Tang, T.-H. Wang, J. Malik, and M. W. Mueller, “A learning-based quadcopter controller with extreme adaptation,” *IEEE Transactions on Robotics*, vol. 41, pp. 3948–3964, 2025.
- [5] J. Eschmann, D. Albani, and G. Loianno, “Learning to Fly in Seconds,” Apr. 2024, arXiv:2311.13081 [cs, eess]. [Online]. Available: <http://arxiv.org/abs/2311.13081>

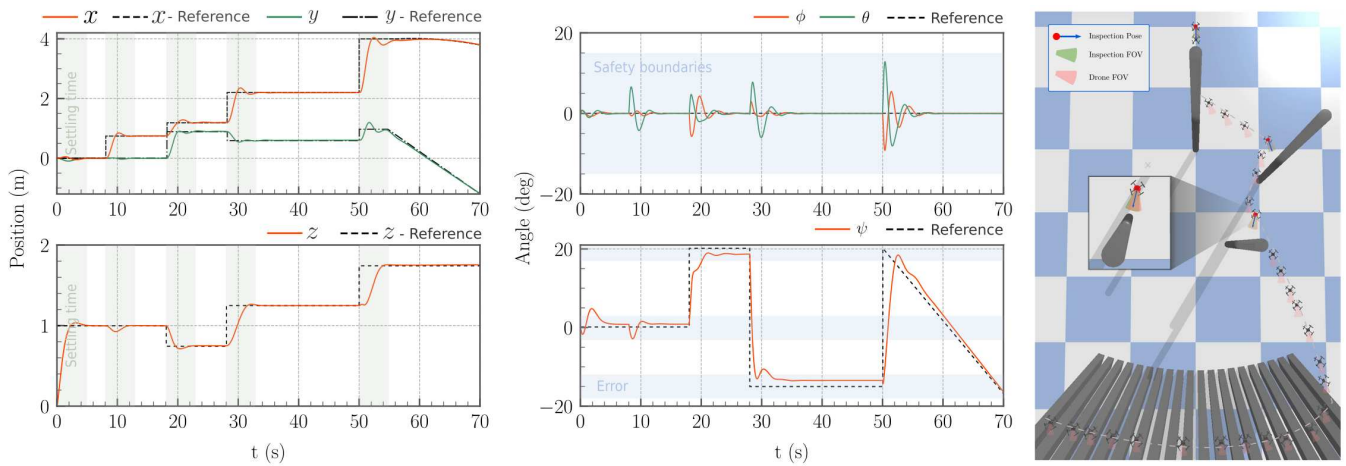


Fig. 9: Over 70 s, the drone inspects three columns at different altitudes and yaw angles, then follows a trajectory parallel to a circular wall, inspecting it while continuously varying its yaw.

- [6] M. Kulkarni, T. J. L. Forgaard, and K. Alexis, "Aerial Gym – Isaac Gym Simulator for Aerial Robots," May 2023, arXiv:2305.16510 [cs]. [Online]. Available: <http://arxiv.org/abs/2305.16510>
- [7] M. Kulkarni, W. Rehberg, and K. Alexis, "Aerial gym simulator: A framework for highly parallelized simulation of aerial robots," *IEEE Robotics and Automation Letters*, vol. 10, no. 4, pp. 4093–4100, 2025.
- [8] C. A. Dimmig, G. Silano, K. McGuire, C. Gabellieri, W. Hönig, J. Moore, and M. Kobilarov, "Survey of simulators for aerial robots: An overview and in-depth systematic comparisons [survey]," *IEEE Robotics & Automation Magazine*, vol. 32, no. 2, pp. 153–166, 2025.
- [9] S. Gronauer, M. Kissel, L. Sacchetto, M. Korte, and K. Diepold, "Using simulation optimization to improve zero-shot policy transfer of quadrotors," in *2022 IEEE/RSJ International Conference on Intelligent Robots and Systems (IROS)*, 2022, pp. 10 170–10 176.
- [10] E. Kaufmann, L. Bauersfeld, and D. Scaramuzza, "A benchmark comparison of learned control policies for agile quadrotor flight," in *2022 International Conference on Robotics and Automation (ICRA)*, 2022, pp. 10 504–10 510.
- [11] A. Dionigi, G. Costante, and G. Loianno, "The power of input: Benchmarking zero-shot sim-to-real transfer of reinforcement learning control policies for quadrotor control," in *2024 IEEE/RSJ International Conference on Intelligent Robots and Systems (IROS)*, 2024, pp. 11 812–11 818.
- [12] M. Ganai, C. Hirayama, Y.-C. Chang, and S. Gao, "Learning stabilization control from observations by learning lyapunov-like proxy models," in *2023 IEEE International Conference on Robotics and Automation (ICRA)*, 2023, pp. 2913–2920.
- [13] J. Eschmann, D. Albani, and G. Loianno, "Raptor: A foundation policy for quadrotor control," 2025. [Online]. Available: <https://arxiv.org/abs/2509.11481>
- [14] W. Xue, H. Wu, H. Ye, and S. Shao, "An Improved Proximal Policy Optimization Method for Low-Level Control of a Quadrotor," *Actuators*, vol. 11, no. 4, p. 105, Apr. 2022, number: 4 Publisher: Multidisciplinary Digital Publishing Institute. [Online]. Available: <https://www.mdpi.com/2076-0825/11/4/105>
- [15] N. Bernini, M. Bessa, R. Delmas, A. Gold, E. Goubault, R. Pennec, S. Putot, and F. Sillion, "A few lessons learned in reinforcement learning for quadcopter attitude control," in *Proceedings of the 24th International Conference on Hybrid Systems: Computation and Control*. Nashville Tennessee: ACM, May 2021, pp. 1–11. [Online]. Available: <https://dl.acm.org/doi/10.1145/3447928.3456707>
- [16] J. Hwangbo, I. Sa, R. Siegwart, and M. Hutter, "Control of a Quadrotor with Reinforcement Learning," *IEEE Robotics and Automation Letters*, vol. 2, no. 4, pp. 2096–2103, Oct. 2017, arXiv:1707.05110 [cs]. [Online]. Available: <http://arxiv.org/abs/1707.05110>
- [17] B. Xu, F. Gao, C. Yu, R. Zhang, Y. Wu, and Y. Wang, "OmniDrones: An Efficient and Flexible Platform for Reinforcement Learning in Drone Control," Sep. 2023. [Online]. Available: <https://arxiv.org/abs/2309.12825v1>
- [18] G. Feng, H. Zhang, Z. Li, X. B. Peng, B. Basireddy, L. Yue, Z. SONG, L. Yang, Y. Liu, K. Sreenath, and S. Levine, "Genloco: Generalized locomotion controllers for quadrupedal robots," in *Proceedings of The 6th Conference on Robot Learning*, ser. Proceedings of Machine Learning Research, K. Liu, D. Kulic, and J. Ichnowski, Eds., vol. 205. PMLR, 14–18 Dec 2023, pp. 1893–1903. [Online]. Available: <https://proceedings.mlr.press/v205/feng23a.html>
- [19] B. Beigomi and Z. H. Zhu, "Towards real-world efficiency: Domain randomization in reinforcement learning for pre-capture of free-floating moving targets by autonomous robots," in *2024 IEEE International Conference on Robotics and Automation (ICRA)*, 2024, pp. 11 753–11 759.
- [20] C. Luis and J. L. Ny, "Design of a Trajectory Tracking Controller for a Nanoquadcopter," Aug. 2016, arXiv:1608.05786 [cs]. [Online]. Available: <http://arxiv.org/abs/1608.05786>
- [21] R. Ferede, G. de Croon, C. De Wagter, and D. Izzo, "End-to-end neural network based optimal quadcopter control," *Robotics and Autonomous Systems*, vol. 172, p. 104588, Feb. 2024. [Online]. Available: <https://www.sciencedirect.com/science/article/pii/S0921889023002270>
- [22] S. Narvekar, "Curriculum Learning for Reinforcement Learning Domains: A Framework and Survey," *Journal of Machine Learning Research* 21, Jul. 2020.
- [23] J. Karlsson, "Task Decomposition in Reinforcement Learning," [Online]. Available: <https://aaai.org/papers/0006-ss94-02-006-task-decomposition-in-reinforcement-learning/>
- [24] G. Kwon, B. Kim, and N. K. Kwon, "Reinforcement Learning with Task Decomposition and Task-Specific Reward System for Automation of High-Level Tasks," *Biomimetics*, vol. 9, no. 4, p. 196, Apr. 2024, number: 4 Publisher: Multidisciplinary Digital Publishing Institute. [Online]. Available: <https://www.mdpi.com/2313-7673/9/4/196>
- [25] Z. Jiang and A. F. Lynch, "Quadrotor motion control using deep reinforcement learning," *Journal of Unmanned Vehicle Systems*, vol. 9, no. 4, pp. 234–251, Dec. 2021. [Online]. Available: <https://cdnsiencepub.com/doi/10.1139/juvs-2021-0010>
- [26] "utiasDSL/gym-pybullet-drones at 627abb314e473eb52fe2a3c7e30df2de0e7ab589." [Online]. Available: <https://github.com/utiasDSL/gym-pybullet-drones>
- [27] "Gymnasium." [Online]. Available: <https://zenodo.org/record/8127025>
- [28] E. C. a. Y. Bai, "PyBullet, a Python module for physics simulation for games, robotics and machine learning," Apr. 2024, original-date: 2011-04-12T18:45:08Z. [Online]. Available: <https://github.com/bulletphysics/bullet3>
- [29] A. Raffin, A. Hill, A. Gleave, A. Kanervisto, M. Ernestus, and N. Dormann, "Stable-baselines3: reliable reinforcement learning implementations," *The Journal of Machine Learning Research*, vol. 22, no. 1, pp. 268:12 348–268:12 355, Jan. 2021.
- [30] M.-C. Popescu, V. E. Balas, L. Perescu-Popescu, and N. Mastorakis, "Multilayer Perceptron and Neural Networks," vol. 8, no. 7, 2009.